# WIND MEASUREMENTS WITH HIGH-ENERGY DOPPLER LIDAR

**Grady J. Koch[a], Michael J. Kavaya[a], Bruce W. Barnes[a], Jeffrey Y. Beyon[b] , Mulugeta Petros[c], Jirong Yu[a], Farzin Amzajerdian[a], and Upendra N. SIngh[a]**

[a]NASA Langley Research Center, Systems Engineering Division, Hampton, Virginia
[b]California State University—Los Angeles, Dept. of Electrical and Computer Engineering
[c]Science and Technology Corporation, Hampton, Virginia

## 1. INTRODUCTION

Coherent lidars at 2-μm wavelengths from holmium or thulium solid-state lasers have been in use to measure wind for applications in meteorology, aircraft wake vortex tracking, and turbulence detection [1,2,3] These field-deployed lidars, however, have generally been of a pulse energy of a few millijoules, limiting their range capability or restricting operation to regions of high aerosol concentration such as the atmospheric boundary layer. Technology improvements in the form of high-energy pulsed lasers, low noise detectors, and high optical quality telescopes are being evaluated to make wind measurements to long ranges or low aerosol concentrations. This research is aimed at developing lidar technology for satellite-based observation of wind on a global scale.

The VALIDAR project was initiated to demonstrate a high pulse energy coherent Doppler lidar. VALIDAR gets its name from the concept of "validation lidar," in that it can serve as a calibration and validation source for future airborne and spaceborne lidar missions. VALIDAR is housed within a mobile trailer for field measurements.

## 2. LIDAR SYSTEM DESIGN

The optical layout of VALIDAR is shown in Figure 1 and a list of specifications is given in Table 1. A detailed description of the laser, optical, and signal processing components has been previously summarized, and is abbreviated here in favor of concentrating on recent measurements results.[4] The basic design of the laser is a Ho:Tm:LuLiF ring oscillator injection seeded by a continuous-wave (CW) single-frequency laser. This CW laser serves as the master oscilltor for the system, providing both the

* *Corresponding author address*: Grady Koch, NASA Langley Research Center, MS 468, Hampton, VA 23681;e-mail:g.j.koch@larc.nasa.gov

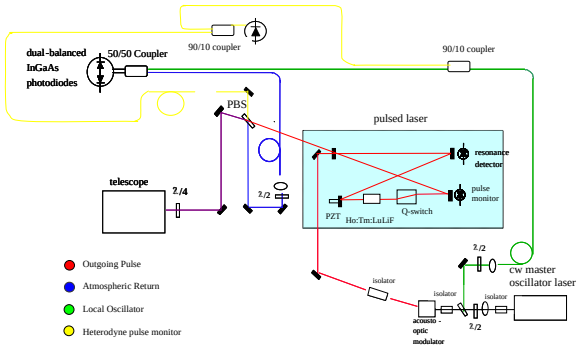


Figure 1: Optical layout of the lidar.

injection seed source and local oscillator for heterodyning. The transmitted and received beams are coaxial, seperated by a polarization relationship imposed by the combinition of a polarizing beam splitter and quarter-wave plate. The output beam is directed through an 8-inch aperture scanner to allowing pointing or scanning to a desired azimuth and elevation. A data acquistion and real-time signal processing system automates control of the scanner, displays data products, and archives data.

## 3. VERTICAL WIND OBSERVATIONS

Profiles are made of vertical wind, as well as cloud and aerosol structure, by pointing the lidar straight up. The atmosphere is continuously sampled, taking an average of 20 pulses over 4 seconds for each profile. Range bins of approximately 150 m with bins overlapping each other by 50% create a data point every 75 m. Sample data includes Figure 2 taken on the gusty afternoon of April 28, 2005. Data is shown over a

| | |
|---|---|
| Laser material | Ho:Tm:LuLiF |
| Pulse energy | 90 mJ |
| Pulse width | 140 ns |
| Pulse repetition rate | 5 Hz |
| Spectrum | single frequency |
| Wavelength | 2053.5 nm |
| Telescope aperture | 6 inches |
| Detector | InGaAs heterodyne |

Table 1: Specifications of VALIDAR

time span of one hour with wind speed and backscatter signal power plotted separately. The signal power shows a typically strong return from the aerosol-rich atmospheric boundary layer (ABL) up to an altitude of approximately 2 km. Above the ABL the aerosol backscatter drops by more than an order of magnitude (a backscatter difference as large as two orders of magnitude between the ABL and free troposphere has been observed in other data). The vertical wind plot shows turbulent motion within the atmospheric boundary layer, but near-zero speed in the free troposphere. Some of the turbulent structure in the boundary layer is seen to be organized in rolling structures. The wind speed shows updrafts and downdrafts, both peaking at 3 m/s, as the roll advects across the view of the lidar. Above these horizontal rolls a series of buoyancy waves was observed with peak speeds of 2 m/s.

Another interesting example of vertical wind structure is shown in Figure 3, taken during a thunderstorm. Various cloud layers are seen in this data, with the early phase of the storm dominated by a low, dense cloud at 1300 m altitude. Under this cloud a sustained updraft reaching 6 m/s occurs as the storm is building up. This updraft subsided and was followed by the low cloud layer breaking up. Rain is seen near the middle of the data set, marked by speeds reaching 12 m/s. This downward speed is believed to be the fall of the rain by gravity enhanced by downdraft pushing the rain drops. Liquid water is effective at absorbing the lidar's energy, and the signal power plot shows a variation in the maximum range as the rate of precipitation varies. Water was also pooling on

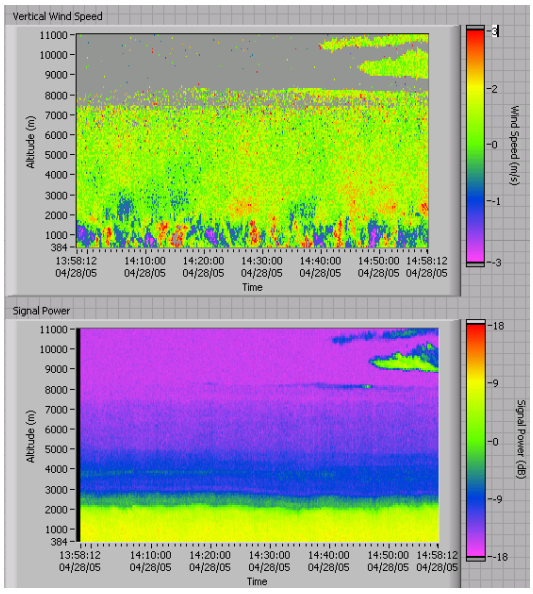


Figure 2: Vertical wind profile over one hour on April 28, 2005.

the output window of the scanner, and the anomaly at 13:44 results from intentionally spinning the scanner to remove the pooled water. The intense rain from this storm quickly dissipated to a relatively calm atmosphere, as seen in the lack of turbulence in the wind speed after 13:45.

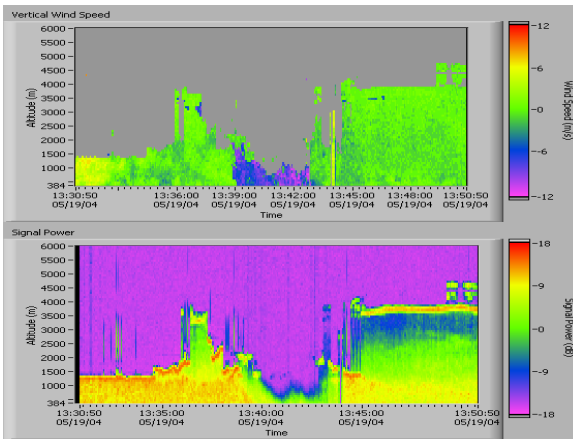


Figure 3: Vertical wind profile taken over 20 minutes on May 19, 2004 during a thunderstorm.

## 4. HORIZONTAL AND VERTICAL WIND OBSERVATIONS

While the vertical wind profiles of the previous section were made with the lidar beam fixed in a zenith viewing angle, the beam can be scanned to various azimuth and elevation angles to measure components of the wind field. These components are vector summed to create a horizontal wind profile. In the following data three scan positions are used: zenith viewing for vertical wind measurements and two orthogonal azimuths at 45 degree elevation for horizontal wind measurements. One set of the three scan directions requires about 30 seconds for pulse averaging, scanner movement, and data archiving. Along each scanner direction 20 pulses are averaged.

Figure 4 is a sample of data taken over a span of almost six hours that shows the formation of a nocturnal jet. Sunset occurred near the middle of this data set. Looking at the vertical wind and backscatter power measurements shows that this was a stable atmosphere with no vertical convection and a lack of low clouds. Though not plotted in Figure 4 in order to emphasize the lower atmosphere, a sub-visible cirrus layer was observed by the lidar in this data at 12 km altitude. The horizontal wind shows speed generally in the 8 m/s range. Early in the

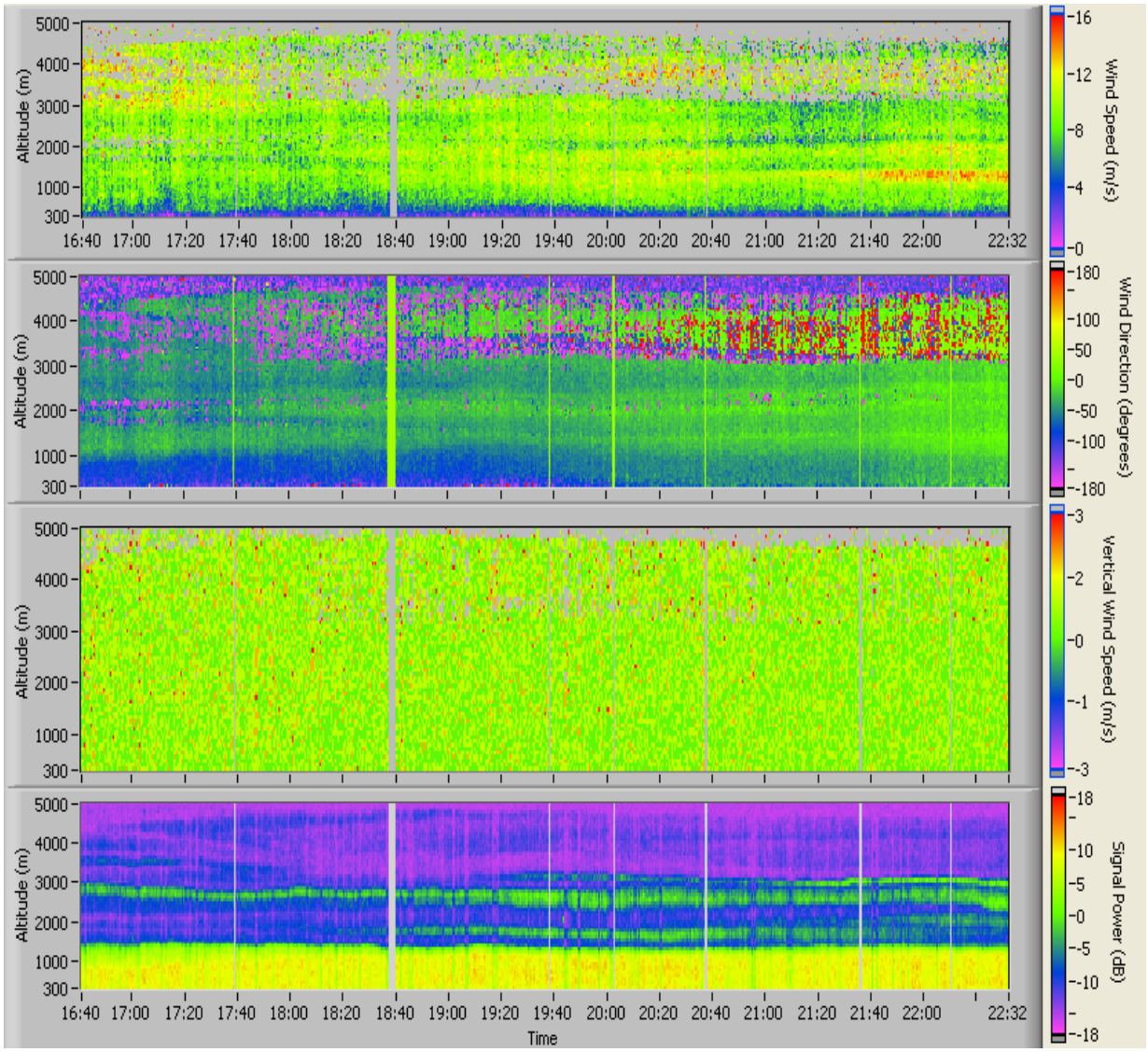


Figure 4: Wind profile taken on the evening of August 23, 2004 showing the formation of a nocturnal jet. Sunset was at 7:45 PM. The panels of data show, from top to bottom, 1) horizontal wind speed, 2) horizontal wind direction, 3) vertical wind speed, and 4) signal power from vertical viewing.

data set, the wind direction is from the west in the ABL, with a shear near the top of the ABL. Above this shear, the wind is from the north in the free troposphere. As the data progresses through sunset the wind shear gradually dissipates to a northerly wind uniform to 5 km altitude. The horizontal speed shows an interesting isolated layer around 1200 m altitude reaching 16 m/s. This nocturnal jet formed at the same altitude at which the wind shear occurred in direction earlier in the data set, that is, near the top of the ABL. A weaker jet peaking at 12 m/s is seen near 2000 m altitude.

Figure 5 shows the wind profiles recorded on June 28, 2005 over a span of 9 ½ hours, with a frontal system passing through in the middle of the data set. The horizontal wind speed within the boundary layer significantly increased with the passage of the front, with the speed peaking in a jet formation of 16 m/s. A shift in the wind direction accompanied the speed increase, moving from southerly to south-westerly flow. Precipitation occurred in the last quarter of the data as shown in the enhanced backscatter of the signal power and has a downward motion reaching as high at 4 m/s. A curious feature of the rain is that the downward motion ceases at an altitude near the transition from the atmospheric boundary layer and the free troposphere, suggesting that the rain evaporates. The lack of rain observed at ground level also indicates that the precipitation was in the form of virga.

## 5. FUTURE WORK

Enhancements to VALIDAR are underway for improved performance and assessment of

technology for an eventual spaceborne instrument, and work has begun on a airborne implementation. Laser technology has advanced at Langley Research Center in higher laser pulse energy, higher efficiency, all-conductive cooling, and ruggedized packaging.[5] Signal processing improvements are being developed for longer range capability and better resolution in both range and velocity.

## 6. REFERENCES


[1] S.M. Hannon, S.W. Henderson, J.A. Thomson, and P. Gatt, "Autonomous lidar wind field sensor: performance predictions," SPIE Volume 2832, pp. 76-91 (1996).

[2] C.J. Grund, R.M. Banta, J.L. George, J.N. Howell, M.J. Post, R.A. Richter, A.M. Weickmann, "High-Resolution Doppler Lidar for Boundary Layer and Cloud Research," J. Atmos. and Ocean. Tech. **18**, 376-393 (2001).

[3] P. Brockman, B.C. Barker, G.J. Koch, D.P.C. Nguyen, and C.L. Britt, "Coherent pulsed lidar sensing of wake vortex position and strength, winds, and turbulence in airport terminal areas." Tenth Biennial Coherent Laser Radar Technology and Applications Coference, pp. 12-15 (1999).

[4] G.J. Koch, M. Petros, B.W. Barnes, J.Y. Beyon, F. Amzajerdian, J. Yu, M.J. Kavaya, and U.N. Singh, "Validar: a testbed for advanced 2-micron Doppler Lidar," SPIE Volume 5412, pp. 87-98 (2004).

[5] M. Petros, J. Yu, S. Chen, U.N. Singh, B.M. Walsh, Y. Bai, and N.P. Barnes, "High-energy diode-pumped Ho:Tm:LuLiF laser for lidar application," SPIE Volume 4893, pp. 203-210 (2003).


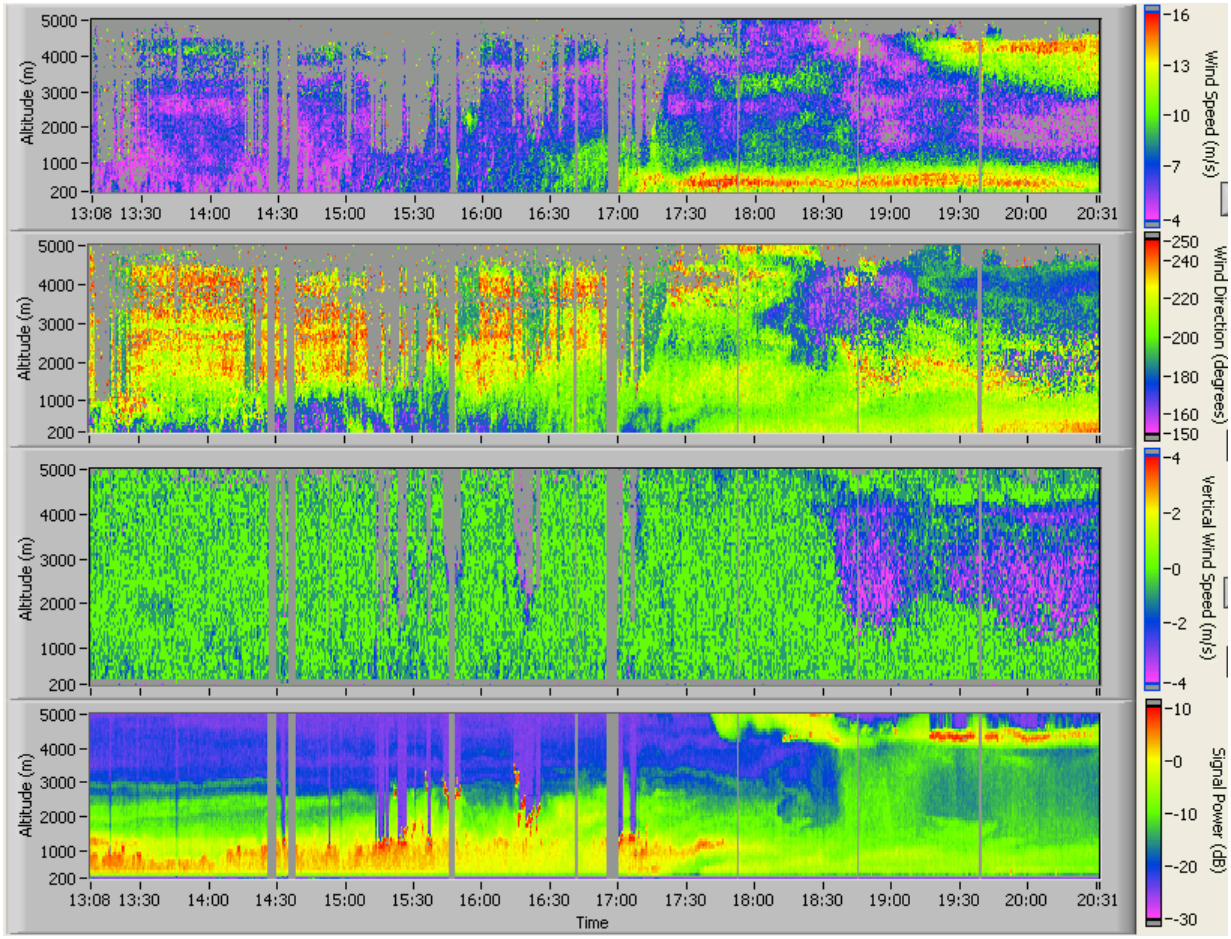


Figure 5: Wind profile taken on June 28, 2005. A weather front passed through in the middle of the data set. The panels of data show, from top to bottom, 1) horizontal wind speed, 2) horizontal wind direction, 3) vertical wind speed, and 4) signal power from vertical viewing.